

REPORT DOCUMENTATION PAGE				<i>Form Approved OMB No. 0704-0188</i>		
<p>The public reporting burden for this collection of information is estimated to average 1 hour per response, including the time for reviewing instructions, searching existing data sources, gathering and maintaining the data needed, and completing and reviewing the collection of information. Send comments regarding this burden estimate or any other aspect of this collection of information, including suggestions for reducing the burden, to Department of Defense, Washington Headquarters Services, Directorate for Information Operations and Reports (0704-0188), 1215 Jefferson Davis Highway, Suite 1204, Arlington, VA 22202-4302. Respondents should be aware that notwithstanding any other provision of law, no person shall be subject to any penalty for failing to comply with a collection of information if it does not display a currently valid OMB control number.</p> <p>PLEASE DO NOT RETURN YOUR FORM TO THE ABOVE ADDRESS.</p>						
1. REPORT DATE (DD-MM-YYYY) 2009		2. REPORT TYPE Reprint		3. DATES COVERED (From - To) Aug 2008-Aug 2009		
4. TITLE AND SUBTITLE Effect of Nano-Aluminum and Fumed Silica Particles on Deflagration and Detonation of Nitromethane				5a. CONTRACT NUMBER W911NF-04-1-0178		
				5b. GRANT NUMBER		
				5c. PROGRAM ELEMENT NUMBER		
6. AUTHOR(S) Justin L. Sabourin a, Richard A. Yetter a, Blaine W. Asay b, Joseph M. Lloyd b, Victor E. Sanders b, Grant A. Risha c, Steven F. Son d				5d. PROJECT NUMBER		
				5e. TASK NUMBER		
				5f. WORK UNIT NUMBER		
7. PERFORMING ORGANIZATION NAME(S) AND ADDRESS(ES) a The Pennsylvania State University, University Park, PA, USA b Los Alamos National Laboratory, Los Alamos, NM, USA c The Pennsylvania State University—Altoona, Altoona, PA, USA d Purdue University, West Lafayette, IN, USA				8. PERFORMING ORGANIZATION REPORT NUMBER		
9. SPONSORING/MONITORING AGENCY NAME(S) AND ADDRESS(ES) U. S. Army Research Office P.O. Box 12211 Research Triangle Park, NC 27709-2211				10. SPONSOR/MONITOR'S ACRONYM(S)		
				11. SPONSOR/MONITOR'S REPORT NUMBER(S)		
12. DISTRIBUTION/AVAILABILITY STATEMENT Approved for public release; federal purpose rights.						
13. SUPPLEMENTARY NOTES The views, opinions and/or findings contained in this report are those of the author(s) and should not be construed as an official						
14. ABSTRACT The heterogeneous interaction between nitromethane (NM), particles of nanoscale aluminum (38 and 80 nm diameter), and fumed silica is examined in terms of the deflagration and detonation characteristics. Burning rates are quantified as functions of pressure using an optical pressure vessel up to 14.2 MPa, while detonation structure is characterized in terms of failure diameter. Nitromethane is gelled using fumed silica (CAB-OSIL), as well as by the nanoaluminum particles themselves. Use of nanoaluminum particles with fumed silica slightly increases burning rates compared to the use of larger diameter Al particles; however distinct increases in burning rates are found when CABO-SIL is removed and replaced with more energetic aluminum nanoparticles, whose high surface area allows them to also act as the gellant. Mixtures including fumed silica yield a reduced burning rate pressure exponent compared to neat NM, while mixtures of aluminum particles alone show a significant increase. Failure diameters of mixture detonations are found to vary significantly as a function of 38 nm aluminum particle loading, reducing more than 50% from that of neat nitromethane with 12.5% (by mass) aluminum loading. Failure diameter results indicate a relative						
15. SUBJECT TERMS Burning Rate, Deflagration, Detonation, Nanoaluminum, Nitromethane						
16. SECURITY CLASSIFICATION OF: a. REPORT UU b. ABSTRACT UU c. THIS PAGE UU			17. LIMITATION OF ABSTRACT UU	18. NUMBER OF PAGES 10	19a. NAME OF RESPONSIBLE PERSON Richard A. Yetter 19b. TELEPHONE NUMBER (Include area code) 814-863-6375	

Reset

Full Paper

Effect of Nano-Aluminum and Fumed Silica Particles on Deflagration and Detonation of Nitromethane

Justin L. Sabourin*, Richard A. Yetter

The Pennsylvania State University, University Park, PA, 16802 (USA)

Blaine W. Asay, Joseph M. Lloyd, Victor E. Sanders

Los Alamos National Laboratory, Los Alamos, NM, 87545 (USA)

Grant A. Risha

The Pennsylvania State University, Altoona, PA, 16601 (USA)

Steven F. Son

Purdue University, West Lafayette, IN, 47907 (USA)

Received: December 03, 2008; revised version: April 27, 2009

DOI: 10.1002/prep.200800106

Abstract

The heterogeneous interaction between nitromethane (NM), particles of nanoscale aluminum (38 and 80 nm diameter), and fumed silica is examined in terms of the deflagration and detonation characteristics. Burning rates are quantified as functions of pressure using an optical pressure vessel up to 14.2 MPa, while detonation structure is characterized in terms of failure diameter. Nitromethane is gelled using fumed silica (CAB-O-SIL®), as well as by the nanoaluminum particles themselves. Use of nanoaluminum particles with fumed silica slightly increases burning rates compared to the use of larger diameter Al particles; however distinct increases in burning rates are found when CAB-O-SIL is removed and replaced with more energetic aluminum nanoparticles, whose high surface area allows them to also act as the gellant. Mixtures including fumed silica yield a reduced burning rate pressure exponent compared to neat NM, while mixtures of aluminum particles alone show a significant increase. Failure diameters of mixture detonations are found to vary significantly as a function of 38 nm aluminum particle loading, reducing more than 50% from that of neat nitromethane with 12.5% (by mass) aluminum loading. Failure diameter results indicate a relative minimum with respect to particle separation (% loading) which is not observed in other heterogeneous mixtures.

Keywords: Burning Rate, Deflagration, Detonation, Nanoaluminum, Nitromethane

1 Introduction

Nitromethane (NM) is a highly energetic, detonatable, liquid organic nitro compound (CH_3NO_2) which may be used as a monopropellant, a bipropellant component, or a high explosive. The non-toxic nature of NM, energy content, low viscosity, ease of manufacture, and handling make it an interesting prospect for present and future propulsion and explosive technologies. Although NM has long been identified as a monopropellant [1, 2], interest in NM has been stagnant until the last decade [3–8] as toxic propellants such as hydrazine are replaced with non-toxic alternatives. As with many liquid mono- and bi-propellants currently in use, or under development, there is interest in improving handling characteristics and energy content by adding a gellant and/or metallic particles. Gelled metallized propellants have long attracted attention from the space exploration and defense communities in search of improved propulsion systems with increased safety and energy density [9]. Gelled propellants share some of the advantageous properties of both liquid and solid propellants. The gelling of liquid mono- and bi-propellants reduces risk of leakages while maintaining their ability to be pumped and throttled, unlike solid propellants. Gelled propellants are generally less sensitive to impact, friction, and electrostatic discharge than solid propellants. Additionally, propellant cracks are a major concern in solid propellants, but are not an issue with gels. From a performance standpoint, gelled propellants

* Corresponding author; e-mail: jls861@psu.edu

offer high specific and density impulses, which are comparable to liquid systems; however, performance may be increased with more energetic materials such as metal particles.

Energy densities of propellants are increased with the addition of metals such as aluminum (Al), which also increase burning rate, due to the exothermic Al oxidation reaction. With the development of nanoparticle manufacturing technologies, researchers have found that burning rates of propellants may be increased further with the use of nanoscale particles [10]. Micron-sized particles, which are used in the majority of metallized propellants, demand longer combustion times for complete combustion and require higher ignition temperatures than smaller nanosized particles. Nanoparticles are desirable since they offer shortened ignition delay, decreased burning times, more complete combustion, higher specific surface area, and the ability to act as gelling agents for liquids, replacing traditionally used low energy gelling agents such as fumed silica (SiO_2). Due to the decreased ignition delay and burning times, nanoparticle reactions contribute more efficiently within the primary reaction zone of liquid propellants, feeding more energy back to the propellant surface, increasing reaction and burning rates of the propellant compared to larger scale metal particles.

The history of experimental and theoretical research of metallized gelled propellants dates back decades, with most of the work devoted to aerospace applications [9, 11]. Much of the work began in the 1950s and 1960s with the study of slurry fuels with various metals. In the 1970s, hydrocarbons, hydrazine derivatives, and inhibited red fuming nitric acid (IRFNA) began to be studied. The majority of the work involving metallized gelled propellants in the last decade and a half has been devoted to bi-propellant systems [12–14], and very few of these studies have involved using nanoscale particles ($d_p < 100 \text{ nm}$) [15]. Recent work has been completed involving the study of metallized gelled nitromethane (NM), using ultra fine aluminum particles (ALEX) from Argonide Corp. (Sanford, FL) and $5 \mu\text{m}$ diameter particles [16]. Although particle size distribution of the ALEX powders was not given, generally they are found to have a relatively large size distribution and a nominal particle diameter greater than 100 nm [17]. Weiser et al. [16] completed theoretical calculations of specific impulse and equilibrium flame temperature, and experimental measurements of flame structure, temperature distribution, and burning rates up to 13 MPa . All mixtures were gelled using Aerosil® 200, which is a commercially available fumed silica. Using 5% Aerosil and ALEX particle loadings of 5 and 10%, burning rates of ~ 4 and 5 mm s^{-1} were found at the highest pressure studied (~ 12 – 13 MPa). Although not stated directly by Weiser et al., it is assumed that the ALEX particle loading is inclusive of oxide coating. From the theoretical calculations, it was determined that flame temperatures (confirmed from experiments) and specific impulse may be increased with aluminum addition to gelled NM. However, above $\sim 5\%$ Al, specific impulse begins to decrease with further loading. In a separate report,

Louaze et al. [18] looked at both the burning rate and flame temperature effects of Aerosil 200 (5, 6, 8 % loading) by itself. Their results showed reductions in mixture burning rates and an increase in pressure dependence with the addition of gelling agent; however the latter result was not conclusive given the uncertainty in the data.

Detonation characteristics of highly energetic heterogeneous mixtures are important from a safety aspect and to the design of future weapon systems. The failure diameter is used as a measure of the ideality of an explosive and is related to the reaction zone length [19] and is a function of many variables. It is known that the addition of an inert material, e.g., glass micro-balloons, has a pronounced effect on the failure diameter of liquid explosives [20]. These inert particles introduce inhomogeneities which produce localized heating (“hot spots”) as opposed to a homogeneous one [21]. This difference results in a very different behavior when measuring the detonation velocity as a function of failure diameter. Heterogeneous materials have large reductions in velocity before failure, while homogeneous explosives have very small deficits. It has been shown that the effect of the added material is a result of a physical effect (local shock heating) rather than a chemical effect (e.g., a surface catalyzed chemical reaction) [22].

The effect of the added inclusions on failure diameter is a function of both the particle density and mixture fraction (and thus the intra-particle spacing) and the bead diameter. If a reactive material is added, rather than an inert material, then one might expect both physical and chemical effects. It is known that the addition of aluminum to explosives increases bubble energies in underwater weapons, raises reaction temperatures, and creates incendiary effects. However, when the particles are large with respect to the reaction zone length, much of the added metal is not consumed in the reaction zone, which yields longer burning times, higher ignition temperatures, and delays. Most of the reaction occurs late in the process, and thus does not contribute directly to the detonation energy. It has been postulated that by incorporating nanoscale metals, the Al reaction will occur in the reaction zone, thus directly feeding energy into the propagating shock wave, and dramatically enhancing detonation performance. The results to date however have been mixed. Brousseau et al. [23] found that nanoaluminum (nAl), 100 – 200 nm in diameter, did not increase the velocity of detonation for a range of plastic-bonded explosives, and in some cases actually decreased performance. However, they found that even if the performance was decreased, in at least one case, the heat of detonation was increased. They also found that when using TNT, nAl increased both the heat of detonation and the detonation velocity, particularly at charge diameters close to the critical diameter, and importantly the failure diameter decreased [23]. LeFrancois et al. [24] found similar results for plastic bonded explosives (100 nm Al) and ascribe the lack of improvement to the large fraction of the Al particle that is present as aluminum oxide. However, they did find that energy release is much better for the explosive containing nAl, which was also found by other workers.

Due to the large specific surface area of the aluminum nanoparticles used, they can simultaneously act as a gelling agent. In this study, NM was gelled with traditionally used fumed silica, as well as solely by the passivated Al particles. The purpose of the current study was to explore the effect of nanoscale metallic particle addition on the combustion characteristics of a liquid monopropellant or explosive, from both a detonation and deflagration perspective. These deflagration and detonation experiments were designed to be an initial survey that when coupled together would provide the basis for more in-depth work to examine effects such as particle size and reaction zone length as well. The reaction zone length of NM detonation has been reported to range between 35 [25] and 200 μm [26], depending on the confinement and other factors, while NM deflagration reaction zone thicknesses have been determined to vary from 900 to 200 μm , at 3 and 15 MPa, respectively, using a detailed model and reaction mechanism [7].

2 Experimental Approach

The effects of the addition of nanoscale aluminum particles to NM were studied in both deflagration and detonation combustion modes in order to determine if, by reducing the size of the Al to the sub-100 nm scale, a positive effect would be obtained. In the deflagration study, burning rates were determined using a large, nearly constant pressure windowed vessel, while detonation characteristics were determined using a conically shaped test fixture to evaluate critical failure diameters.

2.1 Deflagration Study

Over the course of this study two different aluminum nanoparticles were used. The first were 38 nm average diameter particles produced by Technanogy, L.L.C. ($\sim 54\%$ active Al, $54 \text{ m}^2 \text{ g}^{-1}$), the second were 80 nm average diameter particles produced by NovaCentrix, Corp. (formerly Nanotechnologies, Inc., $\sim 81\%$ active Al, $26 \text{ m}^2 \text{ g}^{-1}$). The fumed silicon oxide (CAB-O-SIL[®] TS-720) used was produced by Cabot Corporation and was treated with a dimethyl silicone fluid to increase hydrophobicity, and had a specific surface area of $115 \text{ m}^2 \text{ g}^{-1}$ (BET).

Constituents were measured into small polyethylene bags beginning with all dry components. Mixture weight measurements were made using a Mettler-Toledo analytical balance (AB265-S) with a resolution as low as 0.01 mg. After thoroughly mixing by hand, or in some cases an ultrasonic bath (e.g., low particle concentrations), mixtures were immediately loaded in 10 mm OD (8 mm ID) quartz tubes $\sim 70 \text{ mm}$ long which are capped at one end. Depending on the mixture consistency, a 100 cm^3 syringe, equipped with varying gauges of long hypodermic needles, was employed to load the tube. The syringe allowed for the gel-like mixtures to be loaded with minimal air pockets.

After loading the quartz tubes, air bubbles were removed using vibration and the sample was weighed and measured so that packing density could be determined.

The burning rates of the NM/nAl/CAB-O-SIL mixtures were obtained using an optical pressure vessel (i.e., windowed chamber) under well-controlled operating conditions. The chamber, constructed from 316 stainless steel, is equipped with four optical viewing ports and has a total free volume of 23 l to minimize the pressure variation caused by the generation of gaseous combustion products during an experiment. The optical chamber was brought to the desired initial pressure using argon as the pressurant gas by regulating the inlet and exhaust valves. The continuous purge of argon kept the product gases free from the viewing area. One of the optical viewing ports was backlit using an optical diffuser. The opposite viewing port of the diffuser was used for real-time recording of the burning process with a digital video camera.

The instantaneous pressure was monitored using a Setra 206 pressure transducer. Ignition was obtained by resistance heating either a coiled nichrome wire or a double base booster propellant (NOSOL 363) threaded onto a nichrome wire. Ignition sans propellant was preferred since it was found that the combustion process reaches steady-state quicker; however at low pressure and aluminum loading it was found that the booster was required for ignition. A Nicolet Genesis data acquisition system was used to record the pressure transducer output at a sampling rate of 1000 Hz. The position and time of the regressing luminous front were tracked using the video recorder. From these data, the linear burning rate (r_b) was determined using a curve fit to position vs. time plot, and mass burning rate per unit area was determined by multiplying by the packing density ($m_b = \rho \cdot r_b$). Further details of the strand burner setup may be found in Risha et al. [27].

2.2 Detonation Study

In order to minimize the number of experiments, a conical confinement was used to determine the critical diameter. This method has been used in the past with good results [28, 29]. However, with non-ideal explosives in particular, overdriven detonation processes result in a lower measured failure diameter compared to experiments performed with a constant diameter. Overdriven detonations occur when maximum properties predicted by the Chapman–Jouguet theory are exceeded due to upstream pressures.

All constituents used in failure diameter studies are equivalent to those in the burning rate tests. We experimented with gelling the NM with the addition of 3% by weight of the TS-720 fumed silica to keep the aluminum in suspension. However, we found that the silica had an effect on the failure diameter on its own, and thus we used neat NM and mixed the 38 nm aluminum and initiated the detonation within 5 min to minimize the settling. The mixture was poured into a thin-walled Mylar[®] cone which was placed against a steel witness plate to determine critical

diameter. The mixture was stirred with a long, thin rod as it was poured into the cone to agitate any bubbles to the top.

The cones were made of 0.127 mm thick optically clear Mylar glued together with a 100%-methyl cyanoacrylate (Permabond 910) adhesive. The Mylar film was chosen to minimize the amount of confinement. The cone diameter ranged from 30 mm at the top to 2 mm at the base over a distance of 48.3 cm. Glued to the top of the cone, also with Permabond 910, was a 10.2 cm, 30 mm diameter cylinder (Figure 1) to allow for the development of a steady-state detonation wave. After the mixtures were poured into the cones, a 1.6 mm piece of aluminum sheet was placed over the opening so that the booster was not in direct contact with the NM. A 37 g, 30 mm diameter PBX-9501 booster was glued to aluminum sheet, which was in turn initiated with a standard #8 non-electric detonator. The temperature of the liquid was controlled during the experiments to between 19.0 and 28.4 °C. The temperature was monitored by placing a thermocouple at the top of the cylindrical section, directly into the liquid. As the detonation propagated, it left a roughened section on the witness plate. The point at which the detonation ended was inferred to be the failure diameter.

3 Results and Discussion

3.1 Deflagration Study

Linear and mass burning rate testing included the use of CAB-O-SIL as a gellant due to its high surface area and chain-like structure, making it an excellent thixotrope. However, since the CAB-O-SIL used is primarily made of silica (SiO_2), which lowers the energy density of the mixture,

38 nm Al was used by itself as well, acting as a gellant and significantly increasing energy content of mixture. Although the rheological behavior is not known for NM–nAl mixtures, previous studies of NM and nanoparticles of SiO_2 have shown a shear thinning behavior with yield stress [30].

In order to develop an understanding of the effects of the CAB-O-SIL/NM mixtures alone, initial testing was completed to explore the effect of particle loading on burning rate (Figure 2). Captured images of the burning process for two separate mixtures are illustrated in Figure 3. As in the detonation study, Figure 2 demonstrates that small additions of the oxide gellant (i.e., up to 4–5 wt.-%) affect the combustion process on its own, increasing the burning rates in this case. This would indicate that the heterogeneous interaction between the high surface area particles and NM increases the heat transfer coupling between the condensed

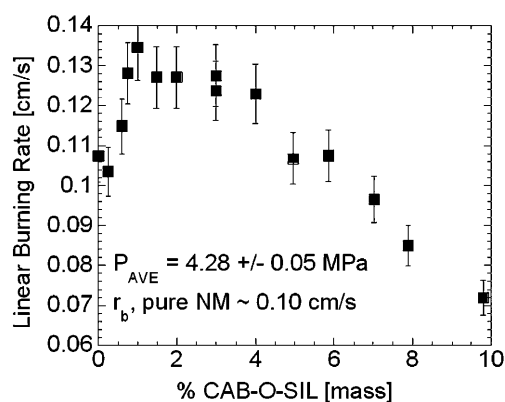


Figure 2. Constant pressure linear burning rate as a function of fumed silica addition.

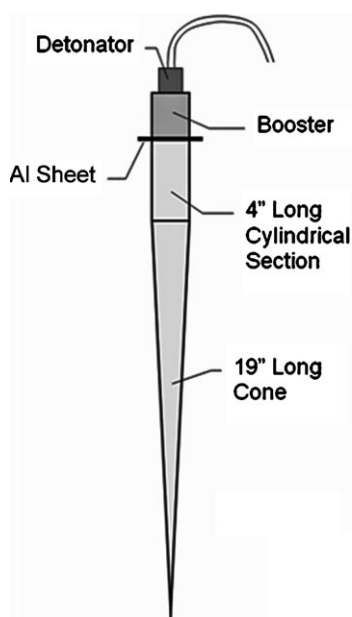


Figure 1. Schematic of cone used to determine failure diameter (not drawn to scale).

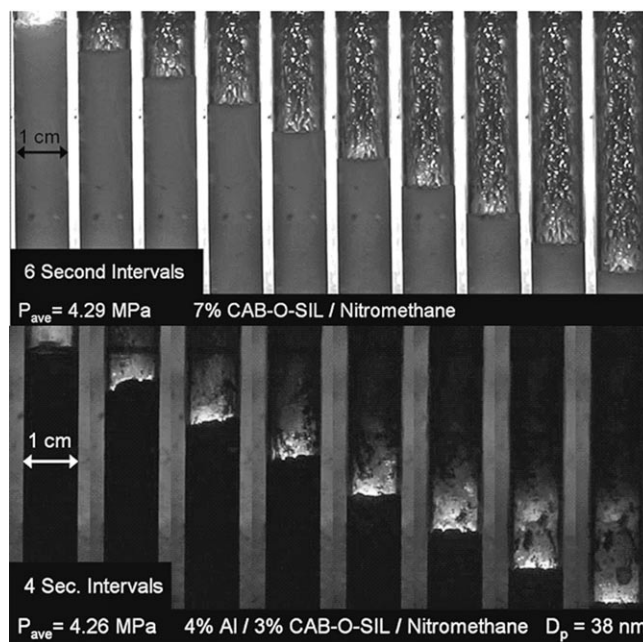


Figure 3. Captured images of deflagration processes.

and gas phases, or affects reaction of the NM itself, such as a possible catalytic effect, enhanced by the extremely high surface area. It can also be expected to affect the thermal diffusivity which would affect burning rate. At higher CAB-O-SIL particle concentrations burning rates are decreased due to lower energy densities (or flame temperature). The latter effect was also observed by Louaze et al. [18], as were long cinders created by coalesced molten silica during the combustion process (Figure 4).

The energetics of the mixtures studied are shown in Table 1. The heat of reaction ($\Delta H_{\text{Reaction}}$) of each individual system is calculated assuming the reaction given in Eq. (1). Equilibrium compositions and mixture enthalpies were calculated using NASA Chemical Equilibrium with Applications (CEA) software [31], assuming a temperature and pressure of 298 K and 1 atm. The diluting effects of the silica are confirmed, as are the enhancing effects of the aluminum.

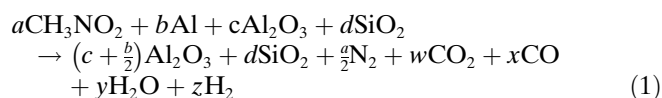


Figure 5 illustrates the results of the burning rates of three different mixtures studied here as a function of pressure. Only the 12.5% 38 nm Al mixture and 4% 38 nm Al/3% CAB-O-SIL mixture may be considered gel-like. The mixture containing the 80 nm particles was much less viscous due to the lower specific area of the particles compared to the 38 nm particles. For comparison, linear burning rates of NM without any additives are shown. Using the burning rate equations developed from the data, which

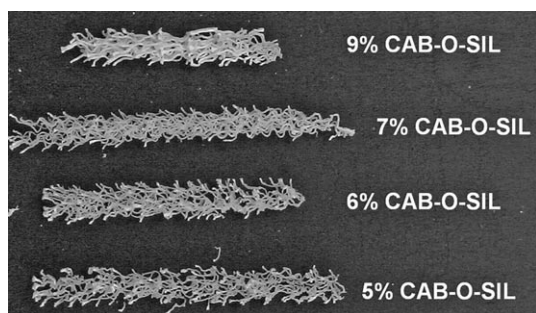


Figure 4. Combustion products of NM and CAB-O-SIL mixtures.

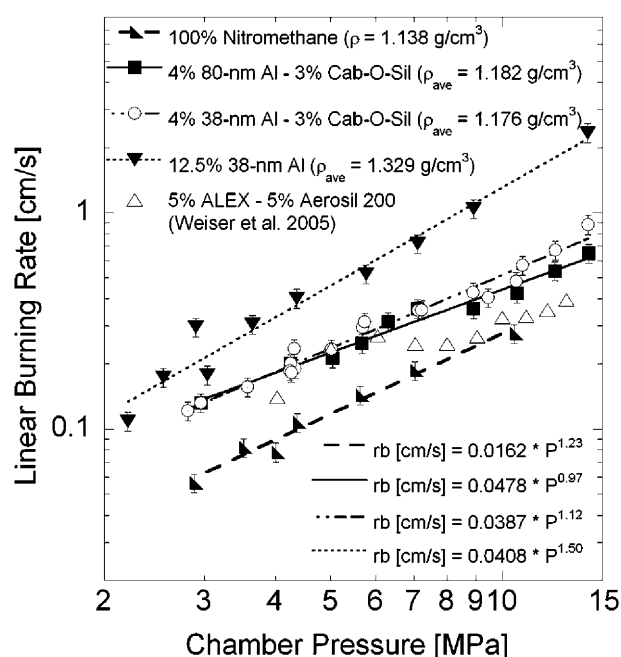


Figure 5. Linear burning rates of various mixtures of NM with nAl particles and fumed silica as a function of pressure (the pure NM case is shown for comparison).

are presented in Figure 5, at a pressure of 5 MPa, the burning rate of pure NM is increased by factors of 2.29 and 3.89 with 4% 38 nm Al (3% CAB-O-SIL) and 12.5% 38 nm Al additions, respectively. In the lower half of the pressure range considered there is little to no difference between the use of 38 and 80 nm diameter particles. Given the burning rates of these mixtures, differences in individual particle burning times between the 38 and 80 nm particles, described by the d^2 -law of diffusion flame theory ($t_{b,diff} \propto d_p^2$) and the d^1 -law for kinetically limited combustion ($t_{b,kin} \propto d_p$) [32], as well as differences in ignition delays and reaction energetics, are not enough to significantly affect burning rates. It should be noted that all mixture percentages are on a mass basis, and all aluminum loadings are exclusive of the oxide coating (i.e., a 12.5% 38 nm Al mixture contains 77% NM and 10.5% Al_2O_3). For this reason the 38 nm particle mixtures contain more alumina than the 80 nm Al particle mixtures. The effects of this on the reaction energetics are shown in Table 1. However, based on the data in Figures 2 and 6, this

Table 1. Combustion energetics of mixtures.

% Al	% SiO_2	Al Particle Size, nm (% Al_2O_3)	$\Delta H_{\text{Reaction}}$ (kJ/gm)	% Deviation from Pure NM
0	0	—	−4.59	—
0	3	—	−4.45	−3.1
1	3	38 (0.84)	−4.53	−1.5
1	3	80 (0.23)	−4.55	−0.9
4	3	38 (3.37)	−4.73	+2.9
4	3	80 (0.94)	−4.84	+5.2
10	3	38 (8.42)	−5.19	+11.6
10	3	80 (2.35)	−5.42	+15.3
12.5	0	38 (10.5)	−5.45	+15.8

difference is not believed to affect burning rates appreciably, and differences in burning rates are attributed more to the particle ignition and burning times. The slight increase in burning rate at higher pressure with decreased particle diameter is ascribed to the reduced flame zone thickness, which reduces the energy contribution of the larger Al particle reactions because of the longer burning time and reduced residence time. Over the range of pressures studied, the predicted combustion zone thickness of NM is reduced by a factor of ~ 4.5 [7].

For comparison, results from Weiser et al. [16] are shown in Figure 5 as well. The Weiser et al. data were obtained using mixtures of 5% ALEX particles and 5% Aerosil 200. This mixture is similar to the 38 and 80 nm CAB-O-SIL mixtures of this study in terms of constituent concentrations. Again, an increase in burning rate is observed with the use of the smaller particles, particularly at high pressures. These results may be explained using the same interpretation as discussed above. Interestingly, if the pure NM data are extrapolated to higher pressures there is little to no difference between the data of Weiser et al. [16], and the pure NM data. This trend may result from the inert gellant addition, which acts as a heat sink and changes phase (i.e., melts) during reaction. In all cases where fumed silica is used the burning rate pressure exponents are less than the pure NM case. The lowest pressure exponent, assuming a power law fit to the Weiser et al. data, occurs with the greatest silica loading. The greatest pressure exponent occurred with 12.5% aluminum loading with no CAB-O-SIL present.

When treated separately, the 4% Al and 3% silica mixtures have two effects. Although the silica acts as a diluent, as Figure 2 shows, burning rates are increased at low concentrations. The aluminum increases the energy content of the system, yielding higher flame temperatures. The small diameter Al nanoparticles contribute to reactions occurring

near the surface as well, increasing the temperature gradient and thus burning rates. Equilibrium predictions, as well as spectroscopic studies indicate that the disparity between neat NM and nAl/NM flame temperatures increases with pressure, which leads to the hypothesis that pressure exponents should increase with Al addition, as seen with the 12.5% Al mixture. When effects of the aluminum and silica particles are combined, the reduction in pressure dependence with these mixtures indicates that the silica alone drives the pressure dependence lower. This may imply that the burning rate pressure exponent of other liquid propellants may be reduced with inert particle addition as well. The mechanism for this may be attributable to a catalytic effect or a physical “flame holding” effect where the gas phase flame is stabilized closer to the surface by solids collecting in the products.

In each case considered above, the effect of aluminum loading was considered as well. At a nominal chamber pressure of ~ 4.3 MPa (625 psi), burning rates were determined as a function of Al concentration (Figures 6 and 7). In Figure 6, a constant CAB-O-SIL loading of 3% (wt.-% of total mixture) is used while varying the aluminum loading up to $\sim 10\%$. For comparison, and to determine effects of aluminum oxide, which is present in large quantities on nanoscale aluminum particles, burning rates of mixtures with pure aluminum oxide are presented as well. Larger aluminum concentrations were not used since the mixture became very thick and clay-like, making loading the quartz sample tube without cracks and air pockets extremely difficult. The plot shows that the smaller Al particles produce greater burning rates, particularly at larger concentrations. As previously indicated, the smaller particles are reacting more efficiently within the flame zone, and contributing more energy to the combustion process. Though there is scatter in the data, it appears as if mass burning rate per unit area exhibits a linear relationship with Al loading. Figure 7 illustrates the effect of aluminum concentration using the 38 nm particles while using no gelling agent. The trends in Figure 6 display noticeable

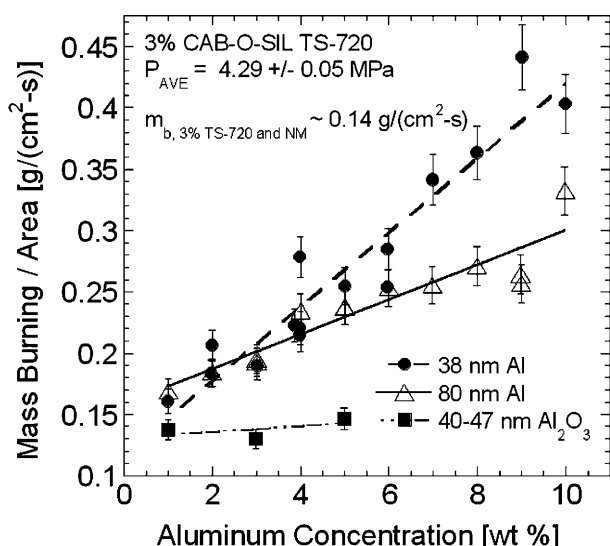


Figure 6. Mass burning rates per unit area of mixtures of NM with 38 and 80 nm Al particles with a constant 3% CAB-O-SIL loading as a function of Al concentration.

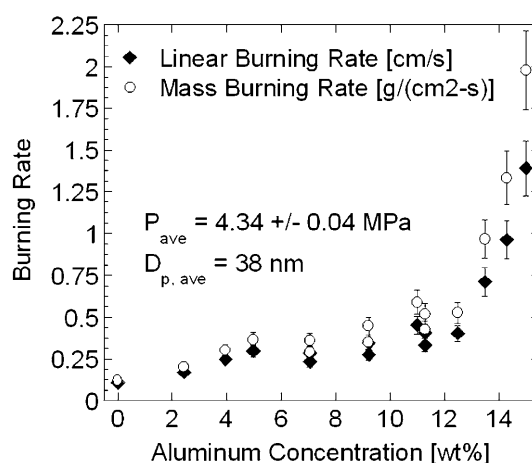


Figure 7. Linear and mass burning rates of mixtures of 38 nm Al particles and NM as a function of Al loading.

differences with that of Figure 7, although a larger range of Al concentrations was studied without the CAB-O-SIL addition. In Figure 7, a linear relationship exists up to 5% Al loading. Above this concentration, the burning rate is less dependent on Al loading until ~13%. For Al loadings greater than 13%, the burning rate increases significantly. The rapid increase above 13% corresponds with a change in mixture consistency from a gel-like to clay-like substance. This results in burning that may not be planar.

As a caveat, long-term particle dispersion is a practical concern at low concentrations of aluminum particles and CAB-O-SIL. In some cases, even when using an ultrasonic bath, significant settling of the mixture may occur. Stratification of aluminum and 3% CAB-O-SIL mixtures was not seen in the time between sample preparation and testing; however, without CAB-O-SIL use, stratification was evident with mixtures below 10% aluminum loading.

3.2 Detonation Study

Figure 8 shows the results of the critical failure diameter study of 38 nm Al and NM mixtures. A common temperature base was obtained by correcting the failure diameter by 0.25 mm/°C to account for the effect of temperature [33]. There is a precipitous drop at approximately 9% Al, with very little effect from 0 to 8%, and a gradual rise from 9%. It is useful to examine the results in a different way using the intra-particle spacing (Eq. (2)) instead of concentration. The results are plotted in Figure 9 along with data from two other studies using inert glass micro-balloons [20, 25]. R is the particle radius, ρ_g is the particle density, W_g is the weight fraction of particles, and ρ is the density of the mixture.

$$L = \left[\frac{4\pi R^3 \rho_g (W_g \rho)^{-1}}{3} \right]^{1/3} \quad (2)$$

Several studies have examined the effect of nAl on detonation performance, but unfortunately as indicated earlier, the results are somewhat ambiguous. Results

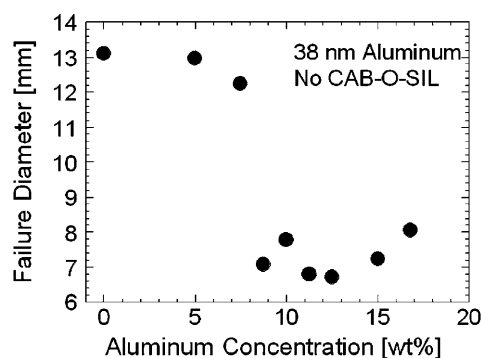


Figure 8. Failure diameter of NM as a function of 38 nm Al concentration.

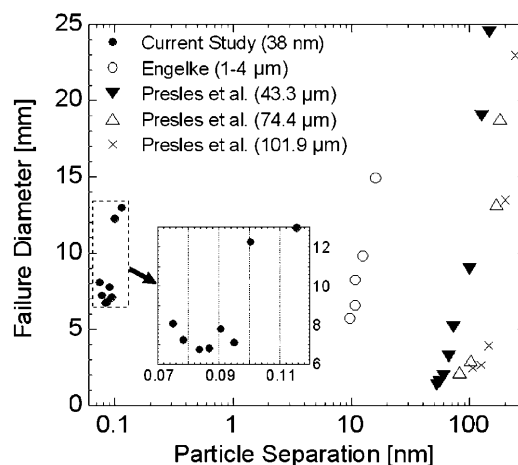


Figure 9. Comparison of NM critical diameter as a function of particle size and concentration. This study used Al, while the other two used glass micro-balloons.

depend strongly on the diameter of the charge, the confinement, the homogeneity of the explosive, reaction zone thickness, particle shape, and size distribution among others that may have not yet been identified. Clearly the addition of Al has similar effects to those found with glass micro balloons. The initial slopes found in Figure 9 are similar among all the different particle sizes. However, our results with aluminum show a minimum while the others do not. The data of Presles et al. [20] show an indication of one, but they did not go high enough in density to have it fully described. Certainly, as the number of particles is increased, the failure diameter must increase, just by dilution effects.

We have demonstrated that the addition of 38 nm aluminum does indeed have a significant effect on the failure diameter; however it appears that the chemical oxidation process is not contributing appreciably to the mechanism driving the detonation; most likely the reaction zone and residence times are too short. Theoretical calculations of the detonation energies using CHEETAH 4.0 software [34] predict a linear increase with aluminum particle addition (Table 2). At 4% 38 nm aluminum particle loading, the thermal detonation energy increases nearly 20%, while the mechanical energy increases by ~7% compared to pure NM. The fact that chemically inactive additives behave similar to reactive particles supports the conclusion that reaction zones are too thin for the aluminum to make appreciable chemical contribution to the detonation process. Additionally, although detonation energies are predicted to increase linearly with Al addition, the failure diameter is highly nonlinear with concentration, again implying that physical rather than chemical interactions are significantly affecting the detonation processes. Using an addition of diethylene triamine or diluants we could adjust the reaction zone thickness independently and repeat the experiments in order to begin to quantify its effect and this is suggested for future work.

Table 2. Theoretical detonation energies.

% Al	% Al ₂ O ₃	Density (g/cm ³)	Thermal detonation energy (kJ/cm ³)	Mechanical detonation energy (kJ/cm ³)	Total detonation energy (kJ/cm ³)
0	0	1.14	−1.68	−6.07	−7.75
4	3.37	1.20	−2.00	−6.50	−8.50
8	6.73	1.26	−2.41	−6.91	−9.32
16	13.5	1.40	−3.30	−7.73	−11.0

4 Conclusions

The deflagration burning rates and detonation critical diameters of NM, metallized with aluminum nanoparticles, illustrate how nanoscale energetic materials may influence combustion processes. The use of metallic nanoparticles to alter liquid propellant energy densities and handling characteristics are described. Linear and mass burning rates of NM gelled with CAB-O-SIL are increased with aluminum particle addition. Rates are further increased with the use of smaller particles, particularly at high pressures where reaction zone thickness is reduced, decreasing the time available for particle burning to contribute flame propagation. Aluminum particles demonstrated the possibility of acting as a gelling agent, removing much, if not all need for non-energetic gellants, such as fumed silica or other oxides. Removing CAB-O-SIL gellant and replacing with aluminum allows for much higher metal loading while maintaining a gel-like consistency, increasing energy densities, burning rates, and pressure sensitivity. Additionally, inert fumed silica addition appears to reduce the burning rate pressure exponent, producing lower pressure sensitivity. Although detonation processes were affected significantly, additions of energetic nanoaluminum particles did not decrease critical failure diameters below levels obtainable using inert particles of larger diameter. The results indicate that detonation reaction zones and time scales are too small for the exothermic nanoparticle reactions to significantly contribute to the detonation process but the particles can induce localized heating (“hot spots”). Primary causes for the reduced failure diameters are therefore attributed to physical effects due to the state dependence of heat release of the heterogeneous mixtures.

In both the detonation and deflagration modes, the significance of reaction zone and particle diameter length scale is emphasized. More information regarding the matching of these scales is needed in order to tailor future propellant and explosive systems.

5 References

- [1] F. Zwicky, C. C. Ross, Nitromethane Excels as Rocket Propellant, *SAE J.* **1949**, 57, 22.
- [2] Anon, Evaluate Nitromethane for Rockets, *Aviation Week* **1949**, 50, 27.
- [3] W. Eckl, V. Weiser, M. Weindel, N. Eisenreich, Spectroscopic Investigation of Nitromethane Flames, *Propellants, Explos., Pyrotech.* **1997**, 22, 180.
- [4] E. Boyer, K. K. Kuo, High-Pressure Combustion Behavior of Nitromethane, *35th AIAA/ASME/SAE/ASEE Joint Propulsion Conference*, Los Angeles, California, USA, June 20–24, **1999**, AIAA Paper 1999–2358.
- [5] S. Kelzenberg, N. Eisenreich, W. Eckl, V. Weiser, Modelling Nitromethane Combustion, *Propellants, Explos., Pyrotech.* **1999**, 24, 189.
- [6] R. N. Mulford, D. C. Swift, Modeling Temperatures of Reacting Nitromethane, *14th Conference of the American Physical Society Topical Group on Shock Compression of Condensed Matter*, Baltimore, Maryland, July 31–August 5 **2005**, AIP Conference Proceedings 845, p. 461.
- [7] E. Boyer, K. K. Kuo, Modeling of Nitromethane Flame Structure and Burning Behavior, *Proc. Comb. Inst.* **2006**, 31, 2045.
- [8] E. Boyer, K. K. Kuo, Characteristics of Nitromethane for Propulsion Applications, *44th AIAA Aerospace Sciences Meeting and Exhibit*, Reno, NV, January 9–12 **2006**, AIAA Paper 2006-361.
- [9] B. Natan, S. Rahimi, The Status of Gel Propellants in Year 2000, in: K. K. Kuo, deLuca, L. (Eds.), *Combustion of Energetic Materials*, Begall House, Boca Raton, FL, USA **2001**.
- [10] M. M. Mench, C. L. Yeh, K. K. Kuo, Propellant Burning Rate Enhancement and Thermal Behavior of Ultra-Fine Aluminum Powders (Alex), *29th International Annual Conference of ICT*, Karlsruhe, Germany, June 30–July 3 **1998**, p. 30/1.
- [11] B. Palaszewski, L. S. Ianovski, P. Carrick, Propellant Technologies: Far-Reaching Benefits for Aeronautical and Space-Vehicle Propulsion, *J. Propul. Power* **1998**, 14, 641.
- [12] E. G. Nieder, C. E. Harrod, D. C. Rapp, B. A. Palaszewski, Metallized Gelled Propellants, Technical Memorandum 105418, **1992**, NASA.
- [13] B. Palaszewski, J. S. Zakany, Metallized Gelled Propellants: Oxygen/RP-1/Aluminum Rocket Heat Transfer and Combustion Measurements, *32nd AIAA/ASME/SAE/ASEE Joint Propulsion Conference*, Lake Buena Vista, Florida, USA, July 1–3, **1996**, AIAA Paper 1996–2622.
- [14] D. G. Pelaccio, B. Palaszewski, R. O’Leary, Preliminary Assessment of Using Gel and Hybrid Propellant Propulsion for VTOL/SSTO Launch Systems, *33rd AIAA/ASME/SAE/ASEE Joint Propulsion Conference*, Seattle, Washington, USA, July 6–9, **1997**, AIAA Paper 1997-3216.
- [15] B. Palaszewski, J. Jurns, K. Breisacher, K. Kearns, Metallized Gelled Propellants Combustion Experiments in a Pulse Detonation Engine, *40th AIAA/ASME/SAE/ASEE Joint Propulsion Conference*, Fort Lauderdale, Florida, USA, July 11–14, **2004**, AIAA Paper 2004-4191.
- [16] V. Weiser, N. Eisenreich, S. Kelzenberg, Y. Plitzko, E. Roth, Influence of ALEX and Other Aluminum Particles on Burning Behavior of Gelled Nitromethane Propellants, *International Autumn Seminar on Propellants, Explosives and Pyrotechnics (IASPEP 2005)*, Beijing, October 25–28, **2005**.
- [17] C. E. Johnson, S. Fallis, A. P. Chafin, T. J. Groshens, K. T. Higa, I. M. K. Ismail, T. W. Hawkins, Characterization of Nanometer- to Micron-Sized Aluminum Powders: Size Distribution from Thermogravimetric Analysis, *J. Propul. Power* **2007**, 23, 669.

- [18] G. Louaze, V. Weiser, E. Roth, Influence of Aerosil on the Combustion of Gelled Nitromethane, *38th International Annual Conference of ICT*, Karlsruhe, Germany, June 26–29, **2007**, p. 92/1.
- [19] A. Campbell, R. Engelke, The Diameter Effect in High Density Heterogeneous Explosives, *6th International Symposium on Detonation*, San Diego, CA, August 24–27, **1976**, p. 642.
- [20] H. N. Presles, P. Vidal, J. C. Gois, B. A. Khasainov, B. S. Ermolaev, Influence of Glass Microballoons Size on the Detonation of Nitromethane Based Mixtures, *Shock Waves* **1995**, *4*, 325.
- [21] R. Engelke, J. Bdzil, A Study of the Steady State Reaction Zone Structure of a Homogeneous and a Heterogeneous Explosive, *Phys. Fluids* **1983**, *26*, 2420.
- [22] R. Engelke, Effect of a Chemical Inhomogeneity on the Steady State Detonation Velocity, *Phys. Fluids* **1980**, *23*, 875.
- [23] P. Brousseau, H. E. Dorsett, M. D. Cliff, C. J. Anderson, Detonation Properties of Explosives Containing Nanometric Aluminum Powder, *12th International Detonation Symposium*, San Diego, CA, August 12–16, **2002**, p. 11.
- [24] A. Lefrançois, G. Baudin, C. Le Gallic, P. Boyce, J. P. Coudoing, Nanometric Aluminum Powder Influence on the Detonation Efficiency of Explosives, *12th International Detonation Symposium*, San Diego, CA, August 12–16, **2002**, p. 22.
- [25] R. Engelke, Effect of the Number Density of Heterogeneties on the Critical Diameter of Condensed Explosives, *Phys. Fluids* **1983**, *26*, 2420.
- [26] R. Engelke, Effect of a Physical Inhomogeneity on the Steady State Detonation Velocity, *Phys. Fluids* **1979**, *22*, 1623.
- [27] G. A. Risha, S. F. Son, R. A. Yetter, V. Yang, B. C. Tappan, Combustion of Nano-Aluminum and Liquid Water, *Proc. Combust. Inst.* **2007**, *31*, 2029.
- [28] G. Baudin, A. Lefrançois, D. Bergues, J. Bigot, Y. Champion, Combustion of Nanophase Aluminum in the Detonation Products of Nitromethane, *11th International Detonation Symposium*, Snowmass, CO, August 30–September 4, **1998**, p. 989.
- [29] I. Jaffe, D. Price, Determination of the Critical Diameter of Explosive Materials, *ARS J.* **1962**, *32*, 1060.
- [30] U. Teipel, U. Förter-Barth, Rheological Behavior of Nitromethane Gelled with Nanoparticles, *J. Propul. Power* **2005**, *21*, 40.
- [31] B. J. McBride, S. Gordon, *Computer Program for Calculation of Complex Chemical Equilibrium Compositions and Applications*, NASA-RP-1311, **1996**.
- [32] I. Glassman, *Combustion*, Academic Press, San Diego **1996**.
- [33] A. Campbell, M. Malin, T. Holland, Temperature Effects in the Liquid Explosive, Nitromethane, *J. Appl. Phys.* **1956**, *27*, 963.
- [34] L. E. Fried, K. R. Glaesemann, W. M. Howard, P. C. Souers, P. A. Vitello, *CHEETAH 4.0 User's Manual*, UCRL-CODE-155944, Lawrence Livermore National Laboratory, **2004**.

Acknowledgements

The research at the Pennsylvania State University and Purdue University was supported by the US. Army Research Office under the Multi-University Research Initiative under Contract No. W911NF-04-1-0178. The support and encouragement provided by Ralph A. Anthenien is gratefully acknowledged.